Front. Med. 2023, 17(4): 781−795
https://doi.org/10.1007/s11684-023-0986-x

RESEARCH ARTICLE

Hyperosmolarity promotes macrophage pyroptosis by driving the glycolytic reprogramming of corneal epithelial cells in dry eye disease

Yu Han, Yu Zhang, Kelan Yuan, Yaying Wu, Xiuming Jin, Xiaodan Huang (✉)

Eye Center, The Second Affiliated Hospital, Zhejiang University School of Medicine, Zhejiang Provincial Key Laboratory of Ophthalmology, Zhejiang Provincial Clinical Research Center for Eye Diseases, Zhejiang Provincial Engineering Institute on Eye Diseases, Hangzhou 310009, China

Abstract **Tear film hyperosmolarity plays a core role in the development of dry eye disease (DED) by mediating the disruption of ocular surface homeostasis and triggering inflammation in ocular surface epithelium. In this study, the mechanisms involving the hyperosmolar microenvironment, glycolysis mediating metabolic reprogramming, and pyroptosis were explored clinically, *in vitro*, and *in vivo*. Data from DED clinical samples indicated that the expression of glycolysis and pyroptosis-related genes, including *PKM2* and *GSDMD*, was significantly upregulated and that the secretion of IL-1β significantly increased. *In vitro*, the indirect coculture of macrophages derived from THP-1 and human corneal epithelial cells (HCECs) was used to discuss the interaction among cells. The hyperosmolar environment was found to greatly induce HCECs' metabolic reprogramming, which may be the primary cause of the subsequent inflammation in macrophages upon the activation of the related gene and protein expression. 2-Deoxy-d-glucose (2-DG) could inhibit the glycolysis of HCECs and subsequently suppress the pyroptosis of macrophages. *In vivo*, 2-DG showed potential efficacy in relieving DED activity and could significantly reduce the overexpression of genes and proteins related to glycolysis and pyroptosis. In summary, our findings suggested that hyperosmolar-induced glycolytic reprogramming played an active role in promoting DED inflammation by mediating pyroptosis.**

Keywords dry eye disease; glycolytic reprogramming; pyroptosis; inflammation; 2-DG

Introduction

Dry eye disease (DED) is one of the most common ocular surface disorders. In China, the prevalence of DED is 5%–50%, while the morbidity is as high as 31.4% [1–3]. Conventional treatments, such as artificial tears or lubricants, can alleviate the symptoms of mild DED. However, for severe DED, steroids and immunosuppressants are required for long-term application with limited efficacy. Furthermore, steroids and immunosuppressants may lead to serious adverse events [4]. Therefore, on the basis of the limitations and side effects of existing treatments, the pathogenesis of DED and novel treatments need to be studied in detail.

Mechanisms causing DED vary, among which hyperosmotic stress and inflammation are the core and marking characteristics of DED [1]. Tear film instability and hypertonic stress can activate the pressure signaling pathways in ocular surface epithelial cells and immune cells, trigger the secretion of pro-inflammatory factors, and lead to the recruitment and activation of immune cells to promote ocular surface inflammation [5,6]. Nevertheless, the specific mechanism of hypertonic stress in the occurrence and development of DED immune inflammation remains unclear.

The epithelial cell, located in the outermost layer of the corneal tissue, is the first cell barrier on the ocular surface [7]. The tear film is in direct contact with the epithelial cells on the ocular surface. It is one of the sources of nutrients for corneal epithelial cells and provides a stable microenvironment for their metabolism [8]. Research on the tear metabolism spectrum of DED patients has identified potential biomarkers and provided new ideas regarding DED metabolomics; e.g., tear film breakup could lead to abnormal glycolysis featured by the

Received March 6, 2022; accepted January 28, 2023
Correspondence: Xiaodan Huang, huangxiaodan@zju.edu.cn

overexpression of tricarboxylic acid (TCA) circulation [9]. Glycolysis, as the main metabolism in ocular surface epithelial cells [10], is involved in the development of several eye diseases, including herpes interstitial keratitis [11] and alkaline burns [12]. Studies have shown that changes in tear film osmotic pressure and the glycolysis of ocular surface epithelial cells may play an important role in promoting DED development.

Monocytes may infiltrate the ocular surface and differentiate into inflammation-related M1 macrophages, which may induce DED by desiccating stress in mice [13]. In a DED mouse model with systemic autoimmune diseases (such as Sjögren's syndrome, and lupus), the corneal stroma, limbus, and lacrimal gland of DED mice have a large number of $CD4^+$ T cells and infiltrate macrophages, while the depletion of local macrophages could significantly improve tear secretion and alleviate DED activity [14]. Macrophages, as the first line of natural defense in ocular surface immunity, play a vital role in the development of ocular surface diseases [15,16].

Emerging evidence has indicated that macrophage pyroptosis is a key factor involved in the inflammation response in different organs, including the central nervous system [17], liver [18], and kidney [19]. Pyroptosis is the programmed cell necrosis response to inflammation. Gasdermin D (GSDMD), cleaved by activated caspase molecules, may change intracellular osmotic pressure and form holes in the cell membrane, which could lead to the release of mature IL-1β and IL-18, thereby triggering cell death and inflammation [20]. Moreover, the activation of macrophage pyroptosis in the cornea has been proven to promote the development of fungal keratitis [21].

Although hypertonic stress, glycolysis, corneal epithelial cells, and macrophages may play major roles in DED inflammation, the mechanism behind the interaction between epithelial and immune cells in DED remains uncertain. In this study, we initially analyzed the expression of genes related to glycolysis and pyroptosis in the eye of DED patients. Then, the coculture system between human corneal epithelial cells (HCECs) and macrophages derived from THP-1 was used to describe how the interaction promoted DED development, notably the hyperosmotic stress involved. *In vivo* experiments were further performed, and inhibitors for glycolysis were used to describe the dominant role of glycolysis in pyroptosis.

Materials and methods

Patients

A total of 36 clinically diagnosed DED patients (11 males, 25 females; mean age ± standard deviation (SD) = 53.28 ± 2.941 years; range = 24–87 years) comprising 72 eyes were enrolled in this study. A total of 32 healthy volunteers (16 males, 16 females; mean age ± SD = 43.13 ± 4.403 years; range 21–90 years) were recruited as the healthy control. This study was approved by the Institutional Review Board, The Second Affiliated Hospital, Medical College of Zhejiang University, Hangzhou, China (2018-027). All participants voluntarily signed the informed consent forms after being provided with a full explanation of the study. The diagnosis criteria of DED included a score of breakup time ⩽ 10 s and a Schirmer test score < 10 mm/5 min [22]. The inclusion criteria were set as follows: all patients had DED-related symptoms for at least 6 months and used only preservative-free artificial tears (topical anti-inflammatory drugs, such as 0.05% cyclosporine A, or steroids were not used). The exclusion criteria included a history of ocular surgery, contact lens use, or ocular therapies other than artificial tears within the last 3 months. Patients were also excluded if they were pregnant, nursing, or lactating or if they had any systemic diseases (e.g., diabetes, heart diseases, and psychosis). The control group volunteers were healthy, had no history of ocular disease or systemic disease, and did not wear contact lenses. The results of the examinations were all within the normal range.

Conjunctival impression cytology (CIC)

The cellulose acetate film was cut into 3 mm × 3 mm × 4.5 mm right-angle trapezoidal paper sheets (the sharp corner was the smooth surface at the lower right corner, and the sharp corner was the rough surface at the lower left corner). The film was then sterilized and kept sealed. The patient took one to two drops of proparacaine hydrochloride eye drops into the conjunctival sac. After 3–5 min, the sterilized film was pressed on the surface of the conjunctiva at 2 mm from the limbus by using a sterile glass rod to absorb the tears in the conjunctival sac. A total of four ocular surface cells from the upper, lower, nasal, and temporal sides of each eye were collected. All samples were transferred into Eppendorf tubes equipped with 1 mL of TRI-Reagent RNA lysis solution and stored at −80 °C for later use.

Tear collection

Tears were collected from healthy and DED patients by using a capillary tear collector from SEINDA (Shandong, China). The capillary tear collector was held in accordance with the instructions for use. The subject was instructed to turn the eye upward, the lower conjunctival fornix was gently pulled, and the capillary tip of the collection head was placed vertically on the lower conjunctival fornix. When tears filled the capillaries at the tip of the collection head, one-time sampling was deemed complete. Tears were sampled 3 times from each eye. All

samples were then transferred into 0.6 mL sterile dry tubes and stored at −80 °C for later use.

Cell culture

HCECs were purchased from Sigma-Aldrich (St. Louis, MO, USA), and THP-1 cells were obtained from the Cell Bank of the Chinese Academy of Sciences (Shanghai, China). Cell lines were authenticated by ATCC. HCECs were cultured in a DMEM/F12 medium (Gibco, Waltham, MA, USA) supplemented with 1% penicillin–streptomycin–glutamine (PSG) and 10% fetal bovine serum (Gibco, Waltham, MA, USA). For the THP-1 cells, an RPMI 1640 medium with 0.05 mM 2-mercaptoethanol (Gibco, Waltham, MA, USA), 10% FBS, and 1% PSG were used as the culture medium. Cells were cultured at 37 °C in a humidified incubator with 5% CO_2.

Indirect coculture cell model

Transwell (Labselect, Anhui, China) with a 0.4 μm polycarbonate membrane was applied in accordance with the manufacturer's protocol (Fig. 4D). HCECs were seeded into the top and bottom chambers of a Transwell insert. The next day, 10 nmol/L 2-deoxy-d-glucose (2-DG) (MCE, HY-13966) or small interfering RNAs (siRNAs) targeting HK1 or PKM2 (Ribobio, Guangzhou, China) was used to pretreat HCECs. After 6 h, the medium was replaced with a hypertonic medium (HM; 450 mOsM) and cultured for 24 h. The THP-1 cells were stimulated with 150 nmol/L phorbol-12-myristate-13-acetate for 2 days to differentiate macrophages and activate them via LPS (500 ng/mL) challenge for 4 h. The top Transwell chamber seeded with HCECs was then directly placed into the plate containing macrophages derived from THP-1 cells for another 24 h of culture. After coculturing, HCECs and macrophages derived from THP-1 cells were collected for further analysis. *In vitro*, before the indirect coculture, HCECs were cultured in DMEM/F12, and THP-1 was cultured in 1640. During the indirect coculture, the HCEC supernatant (DMEM/F12) was collected to replace the THP-1 supernatant (1640) for coculturing.

Animals

Eight-week-old MRL/MPJ and MRL/lpr mice were purchased from Shanghai SLAC Laboratory Animal Co., Ltd. The MRL/MPJ mice served as the negative control. All experiments were performed in accordance with the Institutional Animal Care and User Committee Guidelines of the Second Affiliated Hospital of Zhejiang University (2020-131). The MRL/lpr mice were randomly divided into model and treatment groups, and the treatment group was intraperitoneally injected with 250 mg/kg of 2-DG continuously for 28 days. The model group was injected with 100 μL of normal saline.

Real-time quantitative PCR (RT-qPCR)

Gene expression was analyzed by RT-qPCR with the ViiA™ 7 Real-Time PCR System (Applied Biosystems, Waltham, MA, USA) using SYBR® Premix Ex Taq™ (Takara). cDNA was prepared using a PrimeScript RT Reagent Kit gDNA Eraser (Takara). The primer sequence (Table 1) synthesized by Tsingke Biotechnology Co., Ltd. (Beijing, China) was designed with ThermoFisher Scientific's online OligoPerfect™ Designer software and further verified with NCBI's Primer-BLAST software. The results were normalized to β-actin relative to the control and analyzed using the ΔΔCt method ($2^{-\Delta\Delta Ct}$).

Western blot analysis

Cells or animal tissues were lysed with RIPA lysis buffer (Solarbio, R0020, Beijing, China) for cellular protein extraction with the concentrations determined through the BCA protein assay (Thermo Scientific, UJ292597, CA, USA). Proteins from SDS/PAGE were electrotransferred to a 0.2 μm immobilism-P^{SQ} transfer membrane (Merck Millipore, ISEQ00010, Ireland) by electrophoresis. The membrane was then immunoblotted with specific antibodies. Protein detection was performed using the Universal Hood III (Bio-Rad, 731BR00991, USA) and Clarity Western ECL Substrate (Bio-Rad, 170-5061, Hercules, CA, USA). Antibodies against GSDMD (L60), PKM2 (D78A4), and IL-1β (3A6) were obtained using Cell Signaling Technology (Danvers, MA, USA). Antibodies against Caspase-1 (ab79515), NLRP3 (ab263899), HK1 (ab150423), LDH (ab52488), PFKM (ab204131), and PDH (ab172617) were purchased from Abcam (Cambridge, UK). Band intensities were quantified using Image J software (NIH, USA).

Immunohistochemical (IHC) staining

Mouse cornea staining was used to evaluate tissue macrophage infiltration. Frozen sections (8 μm) of the mouse cornea samples were taken out from a −80 °C freezer, dried for 15 min, fixed in 4% PFA for 15 min, and washed 3 times with PBST for 5 min each time, and the excess moisture was blotted out with filter paper. To each specimen, 20 μL of a blocking solution was added, and the specimen was blocked for 2 h at room temperature. After another three washes, 20 μL of F4/80 antibody was added (Biolegend, San Diego, CA, USA) to each specimen, and the sections were stained and allowed to stand overnight at 4 °C in darkness. After washing, 20 μL of secondary antibody was added to each specimen, which was then incubated for 1 h in darkness at

Table 1 RT-qPCR primer

Gene	Forward primer sequence	Reverse primer sequence
Human-*NLRP3*	5′-GATCTTCGCTGCGATCAACAG-3′	5′-CGTGCATTATCTGAACCCCAC-3′
Human-caspase-1	5′-TTTCCGCAAGGTTCGATTTTCA-3′	5′-GGCATCTGCGCTCTACCATC-3′
Human-*GSDMD*	5′-GTGTGTCAACCTGTCTATCAAGG-3′	5′-CATGGCATCGTAGAAGTGGAAG-3′
Human-*IL-1β*	5′-ATGATGGCTTATTACAGTGGCAA-3′	5′-GTCGGAGATTCGTAGCTGGA-3′
Human-*HK1*	5′-GCTCTCCGATGAAACTCTCATAG-3′	5′-GGACCTTACGAATGTTGGCAA-3′
Human-*TPI1*	5′-CTCATCGGCACTCTGAACG-3′	5′-GCGAAGTCGATATAGGCAGTAGG-3′
Human-*GAPDH*	5′-GGAGCGAGATCCCTCCAAAAT-3′	5′- GGCTGTTGTCATACTTCTCATGG-3′
Human-*PGAM*	5′-TCTGGAGGCGCTCCTATGAT-3′	5′-TCTGTGAGGTCTGCATACCTG-3′
Human-E*NO1*	5′-GCCGTGAACGAGAAGTCCTG-3′	5′-ACGCCTGAAGAGACTCGGT-3′
Human-*PKM2*	5′-ATGTCGAAGCCCCATAGTGAA-3′	5′-TGGGTGGTGAATCAATGTCCA-3′
Mouse-*Nlrp3*	5′-TGTGAGAAGCAGGTTCTACTCT-3′	5′-TGTAGCGACTGTTGAGGTCCA-3′
Mouse-caspase-1	5′-AATACAACCACTCGTACACGTC-3′	5′-AGCTCCAACCCTCGGAGAAA-3′
Mouse-*Gsdmd*	5′-TTCCAGTGCCTCCATGAATGT-3′	5′-GCTGTGGACCTCAGTGATCT-3′
Mouse-*Il-1β*	5′-GAAATGCCACCTTTTGACAGTG-3′	5′-TGGATGCTCTCATCAGGACAG-3′
Mouse-*Pkm2*	5′-CGCCTGGACATTGACTCTG-3′	5′-GAAATTCAGCCGAGCCACATT-3′

room temperature. The specimen was washed 3 times with PBST for 5 min each time. Filter paper was used to absorb water. After the sections were mounted with a medium containing DAPI (Yesen Biotechnology, D6109100, China), the samples were observed and photographed under a fluorescence microscope (Leica TCS SP8 MP, Wetzlar, Germany).

Lactate assay

Lactate concentration was measured using a Lactate Assay Kit (Nanjing Jiancheng, A019-2-1, China) in accordance with the manufacturer's instructions. In a typical procedure, absorbance at $A_{530\ nm}$ was measured to lactate concentrations of cell medium supernatants or animal tissue lysates on a plate reader (SpectraMax M5, Molecular Devices, USA). For cellular lactate, the cell medium supernatant of HCECs was collected, and the lactate concentration in the test samples was calculated as follows:

Lactate concentration (nmol/L) = $(A_{test} - A_{blank}) / (A_{standard} - A_{blank})$ × Standard concentration (3 mmol/L) × Sample dilution factor

For the lactate of animal tissues, the mouse cornea, lacrimal gland, and meibomian gland were sonicated with ice normal saline, and the lactate concentration in the test samples was calculated as follows:

Lactate concentration (nmol/gprot) = $(A_{test} - A_{blank}) / (A_{standard} - A_{blank})$ × Standard concentration (3 mmol/L) × Sample protein concentration (gprot/L)

TUNEL assay

In the cornea tissue sections of mice, dead cells in the tissues were measured using a One Step TUNEL Assay Kit (Beyotime Biotechnology, C1088, China) in accordance with the manufacturer's protocol. Frozen sections were fixed with 4% paraformaldehyde for 1 h and washed with PBS. Then, PBS containing 0.5% Triton X-100 was used for permeabilization. The sections were washed, and the PBS was blotted with filter paper. To the working solution of each specimen, 50 μL of TUNEL was added, and the sections were stained for 1 h at 37 °C in darkness. Afterward, the sections were mounted with a medium containing DAPI (Yesen Biotechnology, D6109100, China). The samples were observed and photographed under a fluorescence microscope (Leica, Wetzlar, Germany).

Tear human IL-1β immunoassay

IL-1β was analyzed using a high-sensitivity enzyme-linked immunosorbent assay (ELISA) with SpectraMax® M5 System (Molecular Devices, San Jose, CA, USA). The tear levels of IL-1β were determined with Quantikine® HS ELISA (R&D Systems, Minneapolis, MN, USA). A total of 36 tear samples from DED patients and 32 tear samples from healthy volunteers were included. The tear samples (5 μL) were diluted with Calibrator Diluent RD5T buffer to 100 μL for assay following the manufacturer's protocols.

Flow cytometry and reactive oxygen species (ROS) detection

An ROS Assay Kit (Beyotime, Shanghai, China) was used to detect the intracellular ROS level. THP-1 cells were incubated with 10 μmol/L DCFH-DA staining

solution in darkness for 20 min at 37 °C. Cells were washed 3 times with a serum-free cell culture medium to sufficiently remove DCFH-DA that did not enter the cells. They were then harvested with 0.05% trypsin-EDTA solution, suspended in a fresh medium, and immediately analyzed with a flow cytometer (Canto, BD, USA; 488 nm laser).

Statistical analysis

Each experiment was repeated 3 times. Data are presented as mean ± SD. Student's *t*-test or one-way ANOVA was performed to compare the differences among the groups. Quantitative results were analyzed using GraphPad Prism 7 (GraphPad Software Inc., San Diego, CA, USA). $P < 0.05$ was considered statistically significant.

Results

Increased titer of IL-1β in tears and enhanced glycolysis and pyroptosis on ocular surfaces in DED patients

Through CIC, we collected epithelial cells from the ocular surface of 36 DED patients and 32 healthy controls. Tears were also collected for IL-1β detection. The titer of IL-1β in tears of the DED group significantly increased compared with that of the control group (Fig. 1A). As shown in Fig. 1B–1K, the expression of pyroptosis-related genes, namely, NLR family pyrin domain containing 3 (*NLRP3*), caspase-1, *GSDMD*, and *IL-1β*, and glycolysis-related genes, namely, hexokinase 1 (*HK1*), triosephosphate isomerase 1 (*TPI1*), glyceraldehyde-3-phosphate dehydrogenase (*GAPDH*), phosphoglycerate mutase 1 (*PGAM*), enolase 1 (*ENO1*), and *PKM2*, in the epithelial cells of DED patients significantly increased compared with that in the control group. Therefore, enhanced glycolysis and pyroptosis, as well as increased titer of IL-1β, were observed in DED patients.

Enhanced glycolysis and pyroptosis-related inflammation in DED mouse model

To further confirm the changes in glycolytic and pyroptosis metabolism, a DED mouse model, MRL/lpr, was used [23,24]. We found that the tear secretion of MRL/lpr mice was significantly reduced compared with that of the control group (Fig. 2A), indicating that MRL/lpr mice were reliable as a mouse DED model. As shown in Fig. 2B, the lactate secretion of the cornea tissues of the DED mice was upregulated compared with that of the control group. In Fig. 2C, pyroptosis-related genes, including *Nlrp3*, caspase-1, *Gsdmd*, and *Il-1β*, were upregulated in the cornea of the DED mice compared with those in the cornea of the control group. Western blot analysis further indicated a significant increase in the protein expression of PKM2 and in the key metabolic enzyme for glycolysis. The expression of the corresponding cleaved proteins encoded by caspase-1, *Gsdmd*, and *Il-1β* in the cornea also significantly increased (Fig. 2D).

Pyroptosis in the cornea of DED mice was analyzed by TUNEL assay. As shown in Fig. 2E, the $TUNEL^+$ cells in the cornea of the DED mice significantly increased compared with those in the cornea of the control group. Glycolytic metabolism and pyroptosis increased and that were involved in DED development. The macrophage is one of the most common inflammatory immune cells of the ocular surface immune response in DED, so we analyzed the M1-macrophage marker F4/80 of cornea tissues from DED mice by IHC staining. The IHC staining results in Fig. 2F demonstrate that compared with that in the cornea of the control group, the F4/80 expression in the cornea of DED mice significantly increased. This finding indicated that the infiltration of macrophages increased and might have led to the immune response of DED. Therefore, infiltrating macrophages might trigger the immune response on ocular surfaces in DED.

Hypertonicity-induced pyroptosis by regulating the glycolytic metabolism of the DED microenvironment model *in vitro*

Hyperosmolarity has been proven to be an important factor in the initiation of ocular surface inflammation in DED patients. In accordance with a previous study, an HM (450 mOsM) was used to stimulate HCECs for 24 h to induce a hypertonic cell model [25]. As shown in Fig. 3A, hypertonic stress could regulate the mRNA expression of gene encoding enzymes in the glycolytic metabolic pathways in HCECs. Among them, the *HK1*, glucose-6-phosphate isomerase (*GPI*), phosphofructo-kinase muscle (*PFKM*), aldolase, fructose-bisphosphate A (*ALDOA*), *TPI1*, *PKM2*, phosphoglycerate kinase 1 (*PGK1*), *PGAM*, and *ENO1* genes were upregulated in the 450 mOsM group cells. On the contrary, these genes were significantly downregulated in the pretreatment of the glycolysis inhibitor 2-DG. Western blot analysis of HK1, PFKM, PKM2, LDH, and PDH showed similar changes (Fig. 3B). Lactic acid secretion could also be inhibited by the 2-DG treatment (Fig. 3C). These results indicated that 2-DG could successfully inhibit the changes in glycolytic metabolism induced by the hypertonic environment in HCECs.

To study the interaction between cells, we applied Transwell to mimic the DED ocular surface microenvironment *in vitro* (Fig. 3D). After coculture for 24 h, both activated THP-1 cells and HCECs were collected for further analysis. As illustrated in Fig. 3E, compared with

the isotonic medium (IM) group, the protein expression of NLRP3, cleaved-caspase-1, cleaved-GSDMD, and cleaved-IL-1β in macrophages (THP-1) cocultured with the HM group supernatant of HCECs significantly increased. Interestingly, compared with the HM group, the expression of pyroptosis-related proteins decreased in macrophages cocultured with 2-DG-pretreated hypertonic supernatant. Massive ROS release is the main

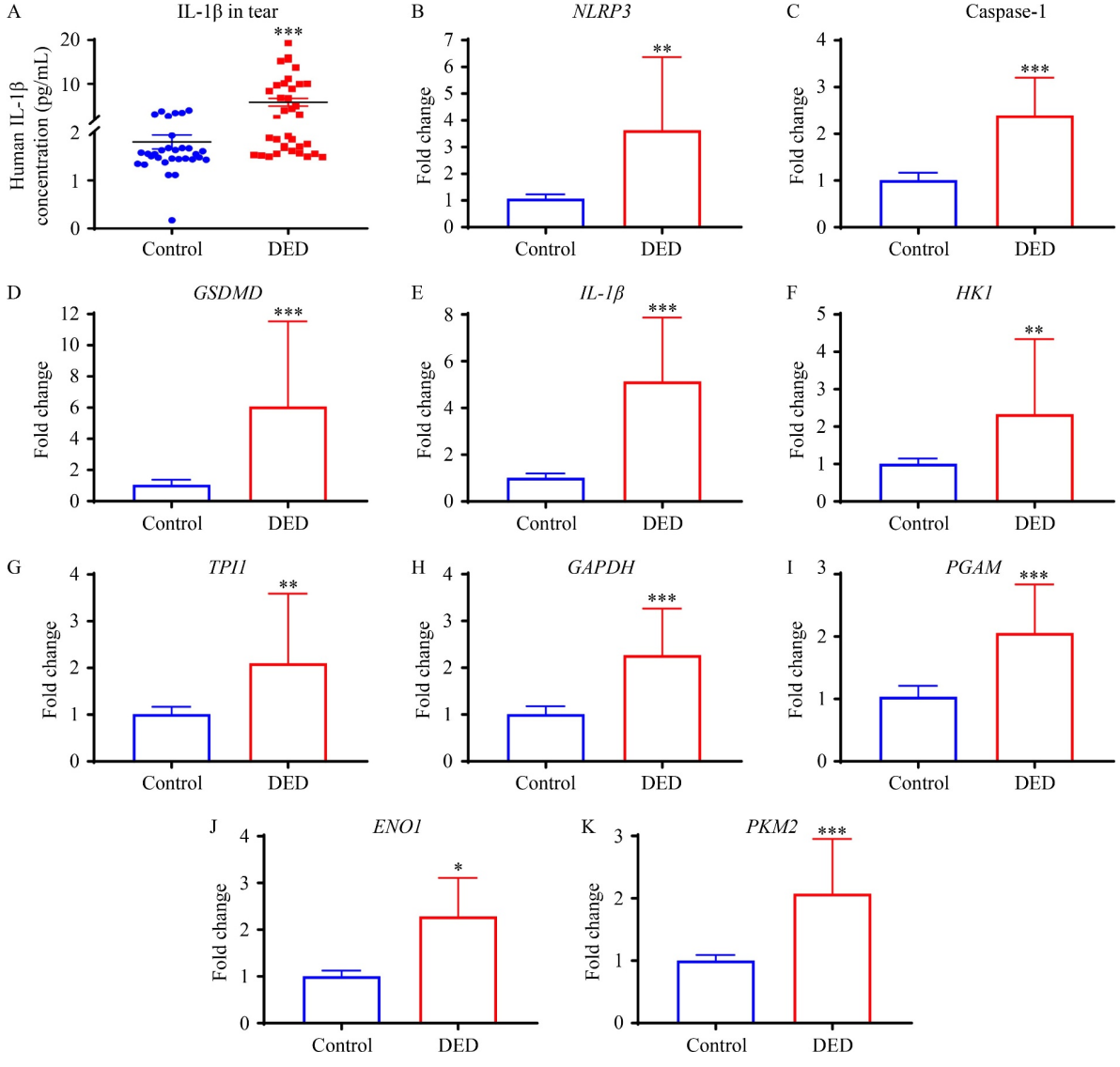

Fig. 1 Study of glycolysis and pyroptosis levels in DED patients. (A) Quantification of IL-1β titer in the tears of DED patients and healthy controls by ELISA. RT-qPCR was used to detect the gene expressions of *NLRP3* (B), caspase-1 (C), *GSDMD* (D), *IL-1β* (E), *HK1* (F), *TPI1* (G), *GAPDH* (H), *PGAM* (I), *ENO1* (J), and *PKM2* (K) in ocular surface cells collected by CIC from DED patients and healthy controls. Data are represented as mean ± SD. *$P < 0.05$, **$P < 0.01$, and ***$P < 0.001$ between the two groups.

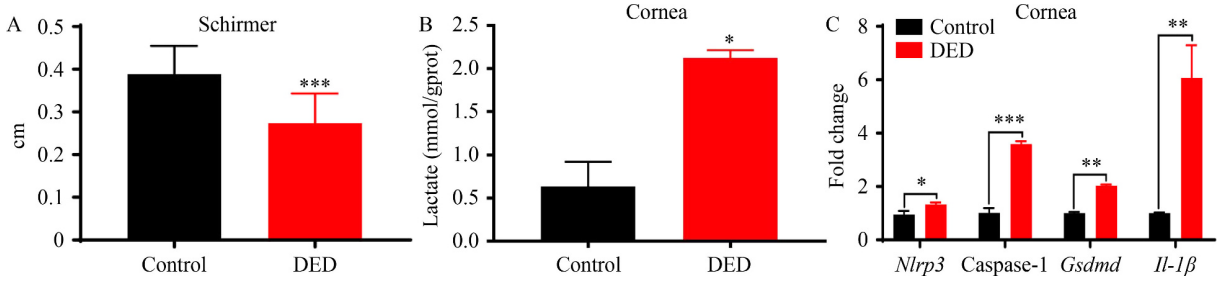

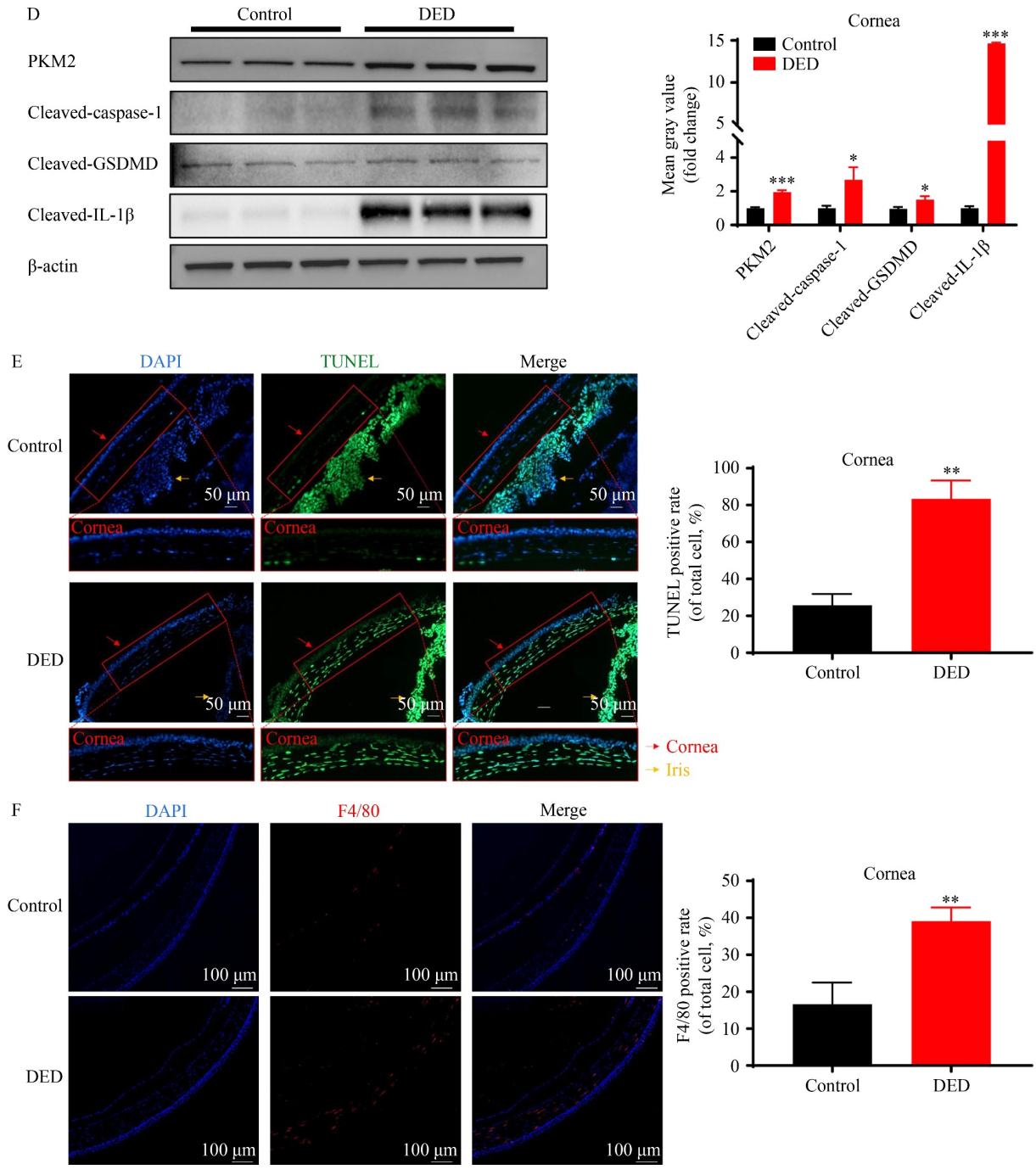

Fig. 2 Glycolysis and pyroptosis level changes in the cornea of the DED mouse model. (A) Tear secretion was examined by the Schirmer test in MRL/MPJ control mice and MRL/lpr DED mice. (B) Lactate concentrations were detected in the cornea by lactate assay. Data were analyzed by *t*-test and are represented as mean ± SD; **P* < 0.05 and ***P* < 0.01. (C) Quantifications of *Nlrp3*, caspase-1, *Gsdmd*, and *Il-1β* gene expressions in the cornea by RT-qPCR. Data were analyzed by one-way ANOVA and are represented as mean ± SD ($n = 3$); * $P < 0.05$, ** $P < 0.01$, and *** $P < 0.001$. (D) Protein expression levels of PKM2, cleaved-caspase-1, cleaved-gasdermin D, and cleaved-IL-1β detected in the cornea by Western blot analysis. The representative immunoblots and protein quantification were analyzed by *t*-test; * $P < 0.05$ and *** $P < 0.001$. (E) TUNEL assay-labeled death cells in mouse cornea; death cells are labeled in green, and cell nucleus are in blue. Scale bar = 50 μm (20×). Quantitation of the ratio of TUNEL positive cells to total cells was performed through TUNEL staining. Data are represented as mean ± SD; ***P* < 0.01, compared with the control group (*t*-test). Representative images (F) of staining macrophages (F4/80, red) infiltrating the mouse corneas. Scale bar = 100 μm (40×). Quantitation of the ratio of F4/80 positive cells to total cells was conducted by IHC staining. Data are represented as mean ± SD; **P* < 0.05, compared with the control group (*t*-test).

characteristic of DED [26], and ROS can activate NLRP3 following the activation of Caspase-1, which causes pyroptosis [27]. The ROS release level of these macrophages (THP-1) was detected by flow cytometry. As presented in Fig. 3F, the ROS release of the macrophages (THP-1) significantly increased in HM compared with that in the IM treatment groups. These data suggested that hyperosmotic stress could mediate glycolytic metabolic reprogramming in HCECs' *in vitro* indirect coculture model, thereby inducing macrophage pyroptosis. Gene silencing by using siRNA, as well by eliminating the interference of 2-DG treatment, was also utilized to study how the glycolysis of HCECs influences the macrophages in a coculture system. Si-RNAs targeting PKM2 (SiPKM2) and HK1 (SiHK1), which are the key factors in the glycolysis pathway, were used to perform post-transcriptional gene silencing (PTGS). The efficiency of transfection was tested by RT-qPCR (Fig. 4A) and lactate secretion (Fig. 4B), which is the initial product of glycolysis process. Western blot

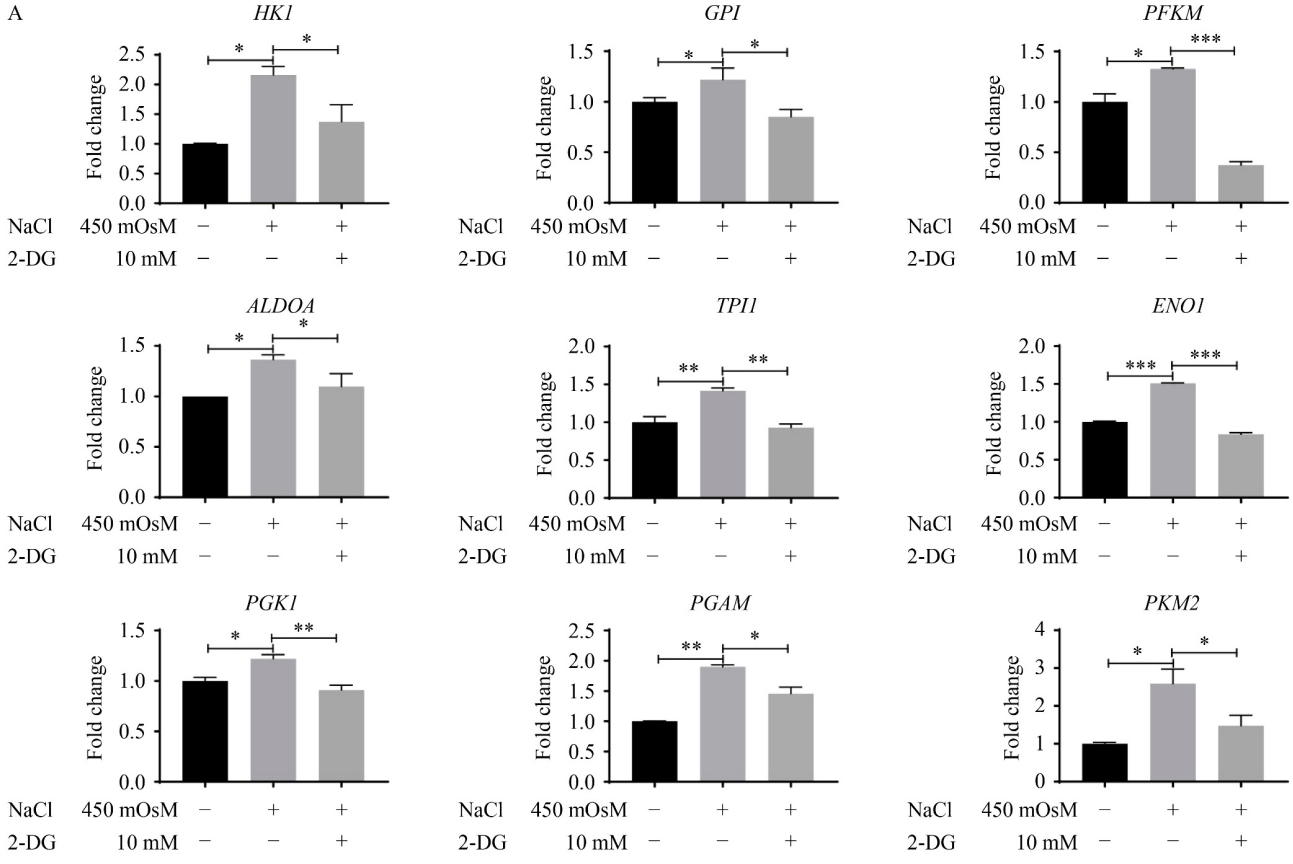

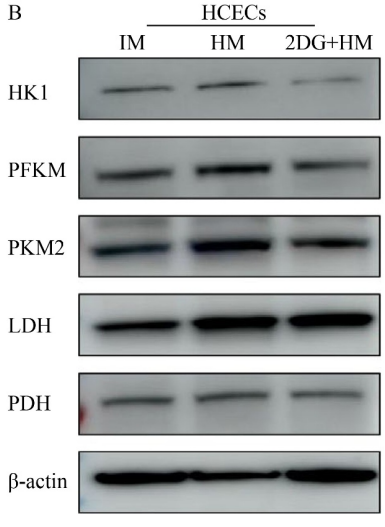

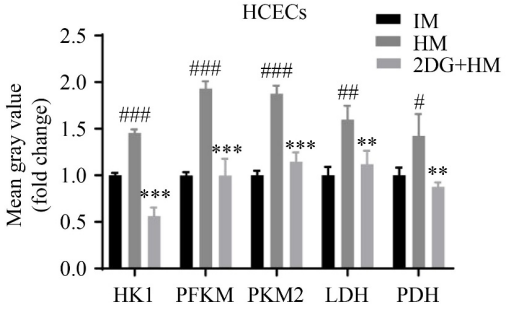

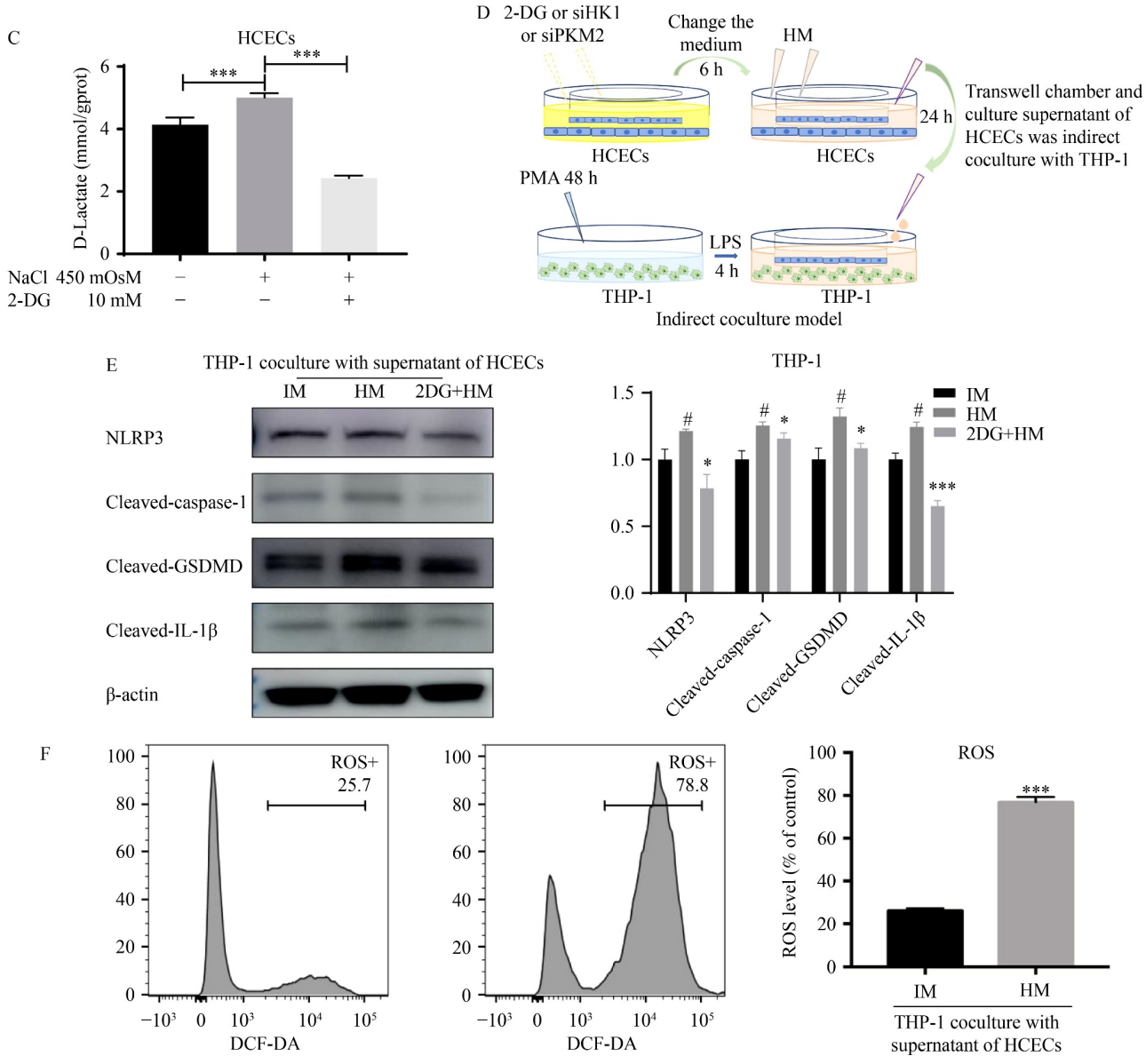

Fig. 3 Regulation effect of glycolysis and pyroptosis in the dry eye microenvironment model *in vitro*. (A) Gene expressions of *HK1, GPI, PFKM, ALDOA, TPI1, ENO1, PGK1, PGAM,* and *PKM2* in HCECs after treatment with 2-DG (10 mM) and HM (450 mOsM). Control cells were cultured in an isotonic medium (IM; 312 mOsM). Data are represented as mean ± SD ($n = 3$); *$P < 0.05$, **$P < 0.01$, and ***$P < 0.001$ (one-way ANOVA). (B) HK1, PFKM, PKM2, LDH, and PDH protein expressions in HCECs after treatment with 2-DG and HM. Data are represented as mean ± SD; *$P < 0.05$ (one-way ANOVA). (C) With or without 2-DG pretreatment, the level of lactic acid secretion was detected in HCEC treatment with HM by ELISA. Data are represented as mean ± SD; **$P < 0.001$ (one-way ANOVA). (D) Schematic of the indirect coculture model of HCECs and THP-1 in a Transwell chamber. (E) Pyroptosis-related protein (NLRP3, cleaved-caspase-1, cleaved-gasdermin D, and cleaved-IL-1β) expression levels in THP-1 examined by Western blot after coculture with HCEC supernatant. The representative immunoblots and protein quantification were analyzed by one-way ANOVA; *$P < 0.05$ and ***$P < 0.001$, compared with HM; $^{\#}P < 0.05$, compared with IM. (F) ROS level of THP-1 examined by flow cytometry after coculture with HCEC supernatant. Data are represented as mean ± SD; ***$P < 0.001$, compared with IM (312 mOsM), *t*-test.

analysis showed that siPKM2 and siHK1 could significantly inhibit the glycolysis of HCECs (Fig. 4C and 4D). In the coculture system, such inhibition of glycolysis could suppress the pyroptosis of macrophage through indirect interaction with HCECs (Fig. 4C and 4D).

Interestingly, we found pyroptotic morphological features in the macrophages treated with HM supernatant of HCECs (Fig. 5A), which could be eliminated by coculturing with the HCECs of inhibited glycolysis. TUNEL (Fig. 5B) and PI (Fig. 5C) staining also indicated that the macrophages' death in the HM supernatant of HCEC treatment could be prevented via coculturing with HCECs of inhibited glycolysis by using an inhibitor or PTGS. Thus, in the DED microenvironment, hypertonic

stress could mediate HCECs' glycolytic metabolism reprogramming, which might be the leading cause of ROS-mediated pyroptosis in macrophages and, ultimately, the inflammation in DED.

2-DG-induced decrease in pyroptosis through glycolysis inhibition in the DED mouse model

To further confirm the regulating effect of glycolysis and pyroptosis in dry eye, we applied the inhibitors in an MRL/lpr mouse model [4,23]. 2-DG was administered by intraperitoneal injection to mice every day at a dose of 250 mg/kg [28]. As shown in Fig. 6A, 2-DG was able to significantly increase tear secretion from week 3 to week 4. The cell death and macrophage infiltration in the cornea of DED mice treated with 2-DG were analyzed by TUNEL and F4/80 staining assays. Compared with the model group, 2-DG reduced the cell death and macrophage infiltration in the cornea of DED mice (Fig. 6B). Western blot analysis of protein lysate from cornea tissues indicated that the expression of PKM2, NLRP3, cleaved-caspase-1, cleaved-GSDMD, and cleaved-IL-1β decreased in the 2-DG group. Thus, inhibiting glycolysis could reduce the occurrence of pyrolysis in the cornea of DED mice. These findings were all supported in DED pathogenesis, and glycolysis was the initial factor mediating the subsequent pyroptosis and inflammation. Inhibiting glycolysis could significantly improve DED in mice (Fig. 6C).

Discussion

The ocular surface microenvironment is complicated and has various components, including ocular surface tissues, extracellular matrix, and immune cells, which can contribute to the maintenance of the microenvironment.

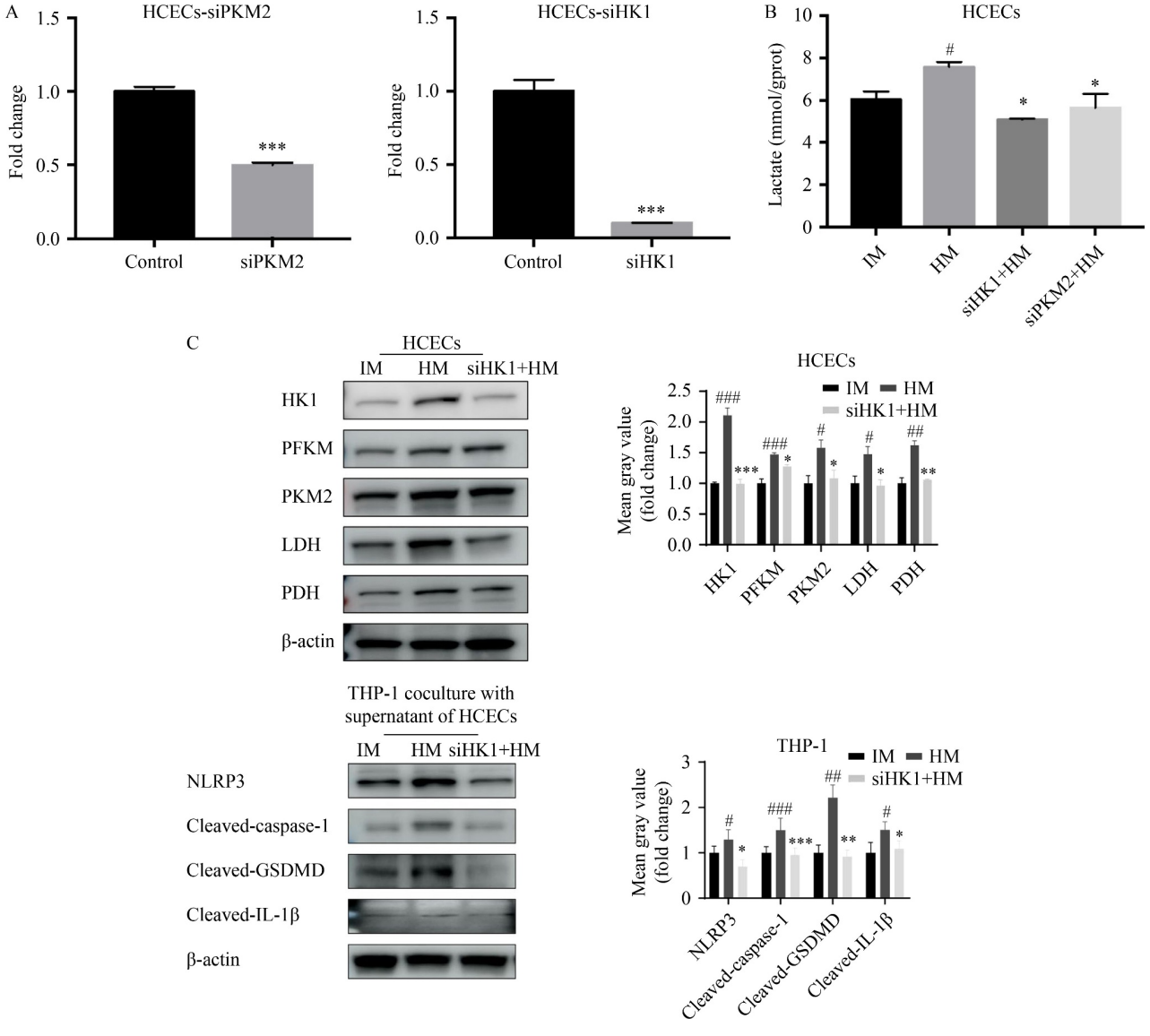

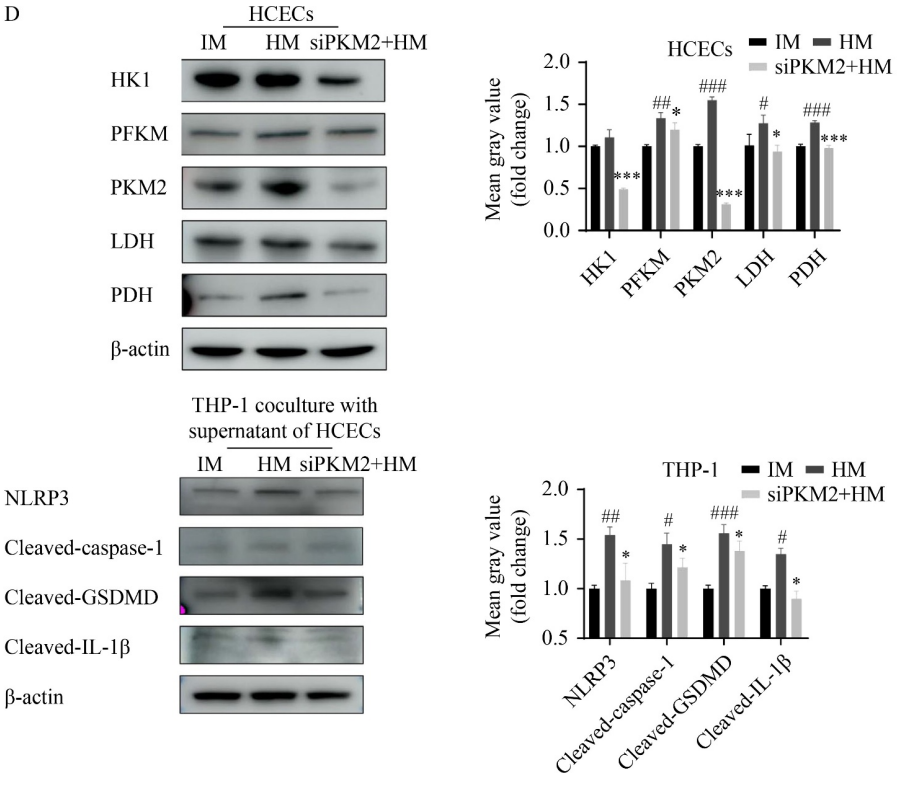

Fig. 4 Level of glycolysis and pyroptosis in the dry eye microenvironment model after siRNA-mediated gene silencing. (A) The expression levels of the targeted genes were knocked down by specific siRNA in HCECs and HCEC-specific gene-knockdown cells. (B) After siRNA-mediated gene silencing, the level of lactic acid secretion was detected in HCEC and HCEC-specific gene-knockdown cell treatments with HM by ELISA. Data were analyzed by one-way ANOVA; $^{*}P < 0.05$, compared with HM; $^{\#}P < 0.05$, compared with IM. (C) Levels of glycolysis (HK1, PFKM, PKM2, LDH, and PDH)-related protein expression in HCECs and pyroptosis (NLRP3, cleaved-caspase-1, cleaved-GSDMD, and cleaved-IL-1β)-related protein expression in macrophages derived from THP-1 after siHK1 treatment and coculture. (D) Level of glycolysis (HK1, PFKM, PKM2, LDH, and PDH)-related protein expression in HCECs and pyroptosis (NLRP3, cleaved-caspase-1, cleaved-GSDMD, and cleaved-IL-1β)-related protein expression in macrophages derived from THP-1 after siPKM2 treatment and coculture. The representative immunoblots and protein quantification were analyzed by one-way ANOVA; $^{*}P < 0.05$, $^{**}P < 0.01$, and $^{***}P < 0.001$, compared with HM; $^{\#\#\#}P < 0.05$, $^{\#\#\#}P < 0.01$, and $^{\#\#\#}P < 0.001$, compared with IM.

The breakdown of the ocular surface microenvironment could ultimately lead to severe DED characterized by inflammatory damage to ocular tissues [29]. Corneal epithelial cells are highly glycolytic and can regulate respiration and glycolysis in accordance with their energy requirements [30,31]. In this study, we collected the ocular surface cells of diagnosed DED patients by CIC and analyzed the expression of related genes by RT-qPCR. We found that the expression of glycolytic enzymes, including *HK1*, *TPI1*, *GAPDH*, *PGAM*, *ENO1*, and *PKM2* (Fig. 1F–1K), significantly increased. This finding proved from a clinical perspective that glycolysis is involved in DED development.

Similar changes were later confirmed *in vivo* by using DED mice. Lactate accumulation (Fig. 2B), pyroptosis (Fig. 2D), and macrophage infiltration (Fig. 2E) in the cornea of DED mice significantly increased. Therefore, glycolysis in epithelial cells and pyrolysis in immune cells contributed to the pathogenesis of DED.

Emerging research has focused on the detailed mechanisms of cells, such as resident epithelial cells and circulating immune cells, as well as their response to disordered microenvironments, whereas few have discussed the interaction between both. We proved the dysfunction of glycolysis in epithelial cells and the overexpression of pyroptosis-related proteins and cytokines induced by macrophages *in vitro* (Figs. 3E, 4C, and 4D). *In vivo*, we found that improving the glycolytic function of DED mice could downregulate the levels of pyroptosis-related factors in the cornea (Fig. 6C). Interestingly, through the coculture of HCECs and macrophages differentiated from THP-1 cells, we found that lactic acid might play a key role in triggering ROS release and could induce inflammation (Fig. 3F). Furthermore, the inhibitor for glycolysis showed potential in relieving DED by inhibiting glycolysis and pyrolysis in the cornea of mice (Fig. 6).

The difference in the metabonomic characteristics of tears of healthy subjects and DED patients was detected, and we found differences in lactate dehydrogenase,

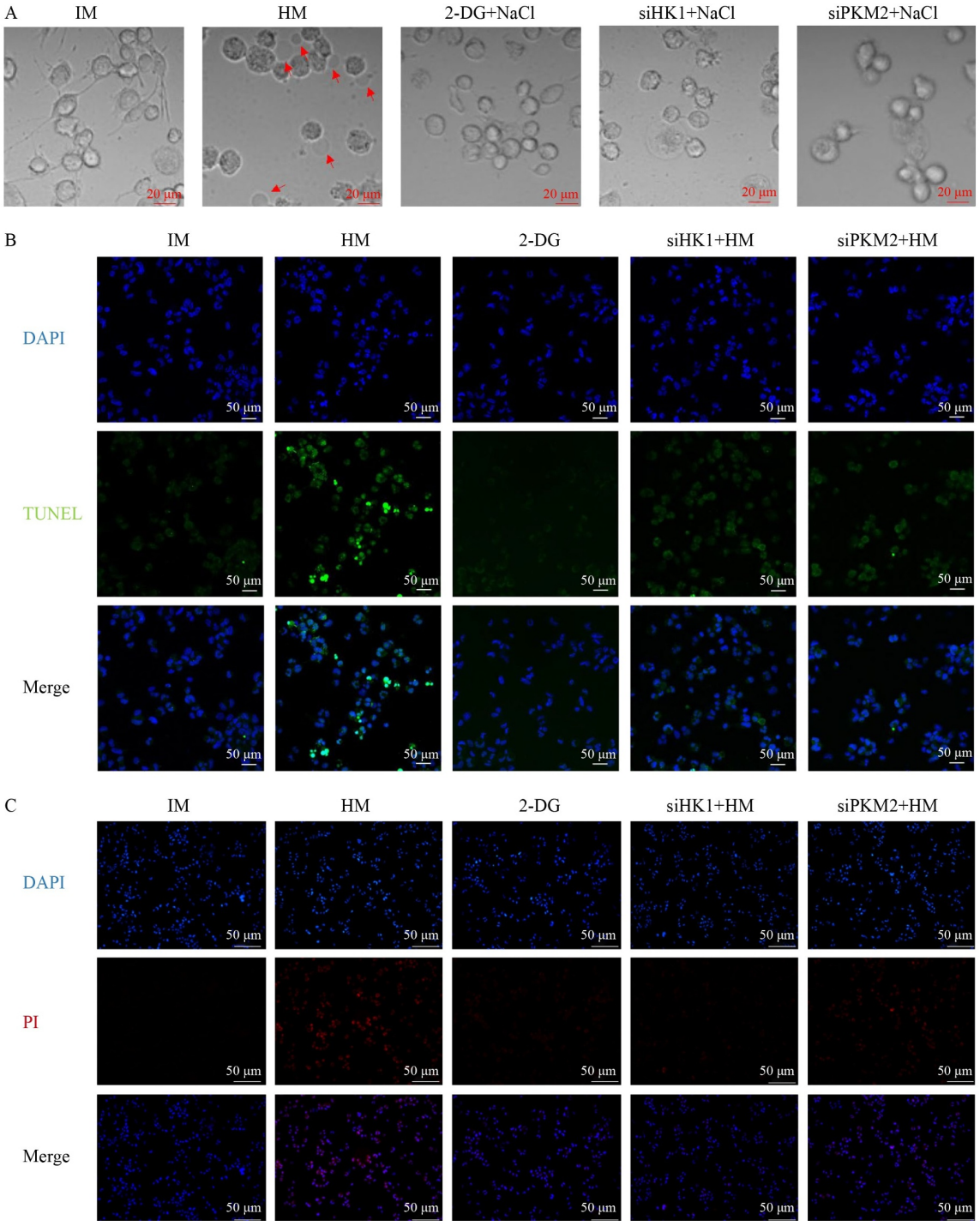

Fig. 5 Level of pyroptosis in THP-1 after inhibiting glycolysis in HCECs in the dry eye microenvironment model. (A) Representative images of THP-1 cells after coculturing with the supernatant of HCECs pretreated with IM, HM, 2-DG, siPKM2, or siHK1 under an optical microscope. The red arrow indicated air bubbles. (B, C) TUNEL and PI staining indicated the cell death of THP-1 in the dry eye microenvironment model. Cell death is labeled in green (TUNEL) and red (PI), and cell nucleus is in blue (DAPI).

glutamate, creatine, and glucose [32]. Lactate, as a metabolite of glycolysis, has long been regarded as a "metabolic waste" and not as a biologically active molecule. However, the accumulation of lactate in the disordered microenvironment has an important regulatory effect on immune cells in the process of residing in and infiltrating [33]. Lactate contributes to the pathogenesis of various diseases [33] and participates in the TCA cycle to provide energy [34]. The acidic environment established by lactate has been reported to enhance the

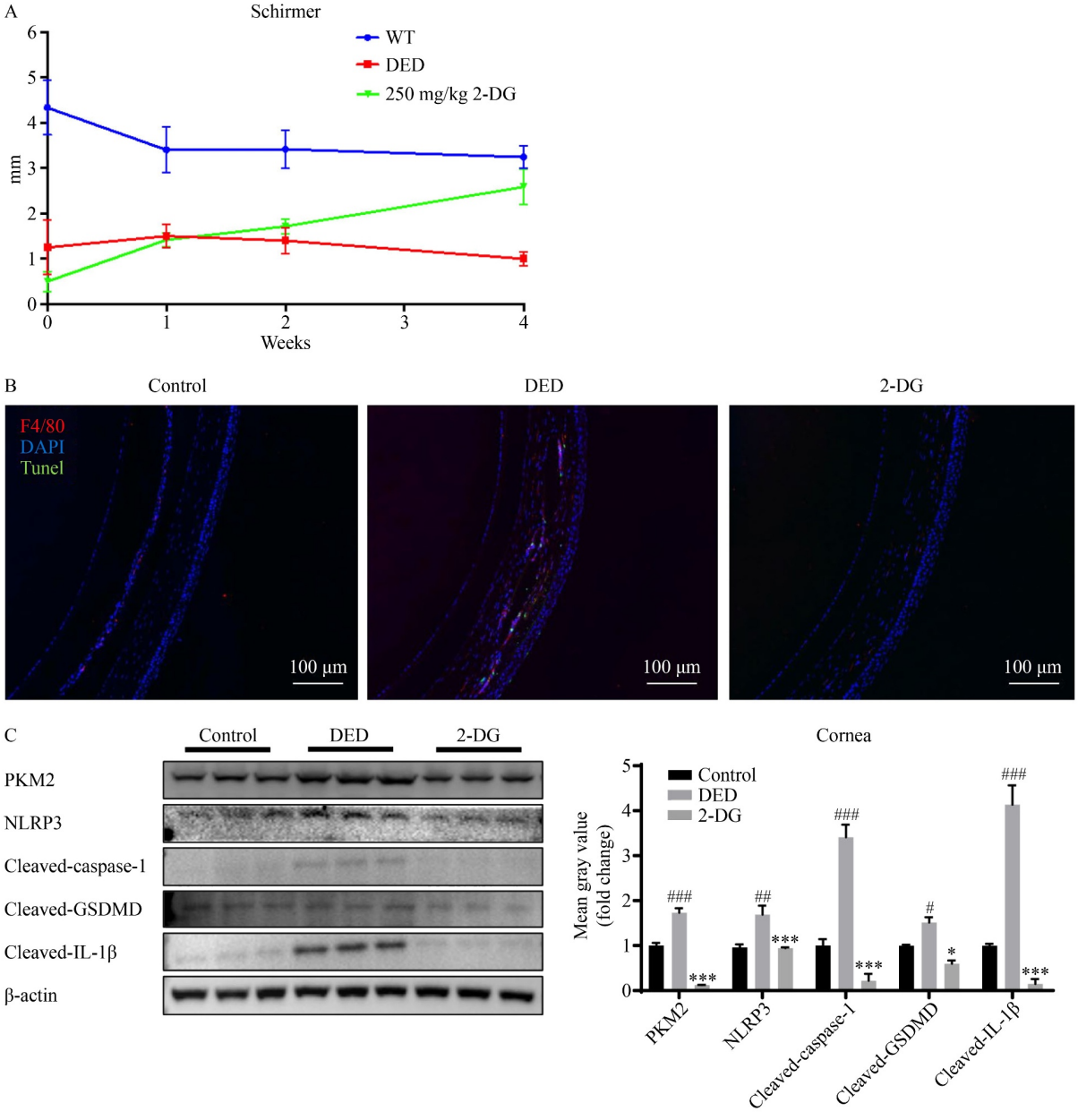

Fig. 6 2-DG inhibited glycolysis and pyroptosis in the cornea of dry eye mice. (A) Treatment of 2-DG (250 mg/kg/day) on tear secretion (Schirmer test) in control and DED mice. (B) Levels of cell death and macrophage infiltration in the cornea of DED mice treated with 2-DG. TUNEL-labeled death cells (green), F4/80-labeled macrophages (red), and DAPI-labeled cell nucleus (blue). Scale bar = 100 μm (40×). Data are represented as mean ± SD; $^{**}P < 0.01$, compared with the control group, *t*-test. (C) 2-DG downregulated the level of pyroptosis through glycolysis inhibition in the cornea of DED mice. Cornea tissue lysates were analyzed by Western blot for PKM2, NLRP3, cleaved-Caspase-1, cleaved-gasdermin D, cleaved-IL-1β, and β-actin (as loading control). Representative Western blots and the protein quantification are shown: $^{###}P < 0.001$, compared with the control group; $^{***}P < 0.001$, compared with DED mice (one-way ANOVA).

production of α-ketoglutarate (α-KG), which was reduced by malate dehydrogenase 1 and converted into L-2HG and ROS, thereby improving the ability of α-KG to induce pyroptosis [35]. Additionally, hyperosmotic stress could induce DED damage by triggering ROS release and apoptosis in the tear film, the key extracellular matrix on the ocular surface [36,37].

The ocular surface inflammation caused by DED includes the innate immunity of epithelial cells and the acquired immunity caused by the infiltration of immune-inflammatory cells. Acquired immunity plays a dominant role. Some existing research has focused on the expression of immunomodulatory molecules in corneal epithelial cells in DED. Studies have shown that NLRP12 and NLRC4 inflammasomes in corneal epithelial cells can induce gasdermin D-dependent pyrolysis and cause

ocular surface epithelial defects in response to hypertonic stress [38]. Moreover, immune cells, including macrophages, as the first natural line of defense for ocular surface immunity, and their role in DED development are undisputed. Nevertheless, the tear film hyperosmotic state can prevent the defense system from functioning [15,16]. In a hypertonic environment, immune cells release pro-inflammatory factors and chemokines, recruit more immune cells, and ultimately lead to a vicious circle of inflammation [6]. Accordingly, a series of DED ocular surface damage and immune-inflammatory responses caused by increased tear film osmotic pressure is involved in multiple cells and tissues. In this study, we used a coculture system of corneal epithelial cells and macrophages to better understand the multicellular environment of the ocular surface of DED (Fig. 3D). To explore the interaction between corneal epithelial cells and ocular surface macrophages in a hypertonic environment, we examined the role played by hypertonic stress-induced changes in corneal epithelial cell glycolysis in ocular surface damage and ocular surface immune inflammation in DED.

Taken together, our findings showed that hypertonic stress mediated the glycolytic reprogramming of ocular surface epithelial cells and promoted the pyroptosis of macrophages via the accumulation of lactic acid in the microenvironment of the ocular surface, thereby promoting DED development inflammation. Our findings suggested the pivotal role of glycolysis-dependent pyroptosis in dry eye. Moreover, compounds capable of modulating the glycolytic pathway are potential pharmacologic candidates for simultaneous use with other conventional drugs, which may provide insights into the search for novel therapeutic strategies and pharmacological targets to improve DED treatment. However, further investigation on the involvement of glycolysis in the corneal epithelium regulating the cellular scorching of immune cells in the pathogenesis of DED is needed.

Acknowledgements

This work was supported by the National Natural Science Foundation of China (Nos. 81870624 and 82171013) and Major Science and Technology Projects of Zhejiang Province (No. 2022C03173).

Compliance with ethics guidelines

Yu Han, Yu Zhang, Kelan Yuan, Yaying Wu, Xiuming Jin, and Xiaodan Huang declare that they have no conflict of interest. All procedures followed were in accordance with the ethical standards of the responsible committee on human experimentation (institutional and national) and with the *Helsinki Declaration* of 1975, as revised in 2000 (5).

References

1. Stapleton F, Alves M, Bunya VY, Jalbert I, Lekhanont K, Malet F, Na KS, Schaumberg D, Uchino M, Vehof J, Viso E, Vitale S, Jones L. TFOS DEWS II epidemiology report. Ocul Surf 2017; 15(3): 334–365
2. Farrand KF, Fridman M, Stillman IÖ, Schaumberg DA. Prevalence of diagnosed dry eye disease in the United States among adults aged 18 years and older. Am J Ophthalmol 2017; 182: 90–98
3. Song P, Xia W, Wang M, Chang X, Wang J, Jin S, Wang J, Wei W, Rudan I. Variations of dry eye disease prevalence by age, sex and geographic characteristics in China: a systematic review and meta-analysis. J Glob Health 2018; 8(2): 020503
4. Jones L, Downie LE, Korb D, Benitez-Del-Castillo JM, Dana R, Deng SX, Dong PN, Geerling G, Hida RY, Liu Y, Seo KY, Tauber J, Wakamatsu TH, Xu J, Wolffsohn JS, Craig JP. TFOS DEWS II management and therapy report. Ocul Surf 2017; 15(3): 575–628
5. Pflugfelder SC, de Paiva CS. The pathophysiology of dry eye disease: what we know and future directions for research. Ophthalmology 2017; 124(11): S4–S13
6. Dai Y, Zhang J, Xiang J, Li Y, Wu D, Xu J. Calcitriol inhibits ROS-NLRP3-IL-1β signaling axis via activation of Nrf2-antioxidant signaling in hyperosmotic stress stimulated human corneal epithelial cells. Redox Biol 2019; 21: 101093
7. Meng YF, Pu Q, Dai SY, Ma Q, Li X, Zhu W. Nicotinamide mononucleotide alleviates hyperosmolarity-induced IL-17a secretion and macrophage activation in corneal epithelial cells/macrophage co-culture system. J Inflamm Res 2021; 14: 479–493
8. Holly FJ, Lemp MA. Tear physiology and dry eyes. Surv Ophthalmol 1977; 22(2): 69–87
9. Jiang Y, Yang C, Zheng Y, Liu Y, Chen Y. A set of global metabolomic biomarker candidates to predict the risk of dry eye disease. Front Cell Dev Biol 2020; 8: 344
10. Riley MV. Glucose and oxygen utilization by the rabbit cornea. Exp Eye Res 1969; 8(2): 193–200
11. Rao P, Suvas S. Development of inflammatory hypoxia and prevalence of glycolytic metabolism in progressing herpes stromal keratitis lesions. J Immunol 2019; 202(2): 514–526
12. Chayakul V, Reim M. The enzymatic activities in the alkali-burnt rabbit cornea. Graefes Arch Clin Exp Ophthalmol 1982; 218(3): 145–148
13. You IC, Coursey TG, Bian F, Barbosa FL, de Paiva CS, Pflugfelder SC. Macrophage phenotype in the ocular surface of experimental murine dry eye disease. Arch Immunol Ther Exp (Warsz) 2015; 63(4): 299–304
14. Zhou D, Chen YT, Chen F, Gallup M, Vijmasi T, Bahrami AF, Noble LB, van Rooijen N, McNamara NA. Critical involvement of macrophage infiltration in the development of Sjögren's syndrome-associated dry eye. Am J Pathol 2012; 181(3): 753–760
15. Yu L, Yu C, Dong H, Mu Y, Zhang R, Zhang Q, Liang W, Li W, Wang X, Zhang L. Recent developments about the pathogenesis of dry eye disease: based on immune inflammatory mechanisms. Front Pharmacol 2021; 12: 732887
16. Milner MS, Beckman KA, Luchs JI, Allen QB, Awdeh RM, Berdahl J, Boland TS, Buznego C, Gira JP, Goldberg DF, Goldman D, Goyal RK, Jackson MA, Katz J, Kim T, Majmudar

PA, Malhotra RP, McDonald MB, Rajpal RK, Raviv T, Rowen S, Shamie N, Solomon JD, Stonecipher K, Tauber S, Trattler W, Walter KA, Waring GO 4th, Weinstock RJ, Wiley WF, Yeu E. Dysfunctional tear syndrome: dry eye disease and associated tear film disorders—new strategies for diagnosis and treatment. Curr Opin Ophthalmol 2017; 27(Suppl 1): 3–47

17. Wang S, Yuan YH, Chen NH, Wang HB. The mechanisms of NLRP3 inflammasome/pyroptosis activation and their role in Parkinson's disease. Int Immunopharmacol 2019; 67: 458–464
18. Wree A, Eguchi A, McGeough MD, Pena CA, Johnson CD, Canbay A, Hoffman HM, Feldstein AE. NLRP3 inflammasome activation results in hepatocyte pyroptosis, liver inflammation, and fibrosis in mice. Hepatology 2014; 59(3): 898–910
19. Lorenz G, Darisipudi MN, Anders HJ. Canonical and non-canonical effects of the NLRP3 inflammasome in kidney inflammation and fibrosis. Nephrol Dial Transplant 2014; 29(1): 41–48
20. Kovacs SB, Miao EA. Gasdermins: effectors of pyroptosis. Trends Cell Biol 2017; 27(9): 673–684
21. Ji Q, Wang L, Liu J, Wu Y, Lv H, Wen Y, Shi L, Qu B, Szentmáry N. *Aspergillus fumigatus*-stimulated human corneal epithelial cells induce pyroptosis of THP-1 macrophages by secreting TSLP. Inflammation 2021; 44(2): 682–692
22. Wolffsohn JS, Arita R, Chalmers R, Djalilian A, Dogru M, Dumbleton K, Gupta PK, Karpecki P, Lazreg S, Pult H, Sullivan BD, Tomlinson A, Tong L, Villani E, Yoon KC, Jones L, Craig JP. TFOS DEWS II diagnostic methodology report. Ocul Surf 2017; 15(3): 539–574
23. Gao J, Morgan G, Tieu D, Schwalb TA, Luo JY, Wheeler LA, Stern ME. ICAM-1 expression predisposes ocular tissues to immune-based inflammation in dry eye patients and Sjögrens syndrome-like MRL/lpr mice. Exp Eye Res 2004; 78(4): 823–835
24. Ma X, Zou J, He L, Zhang Y. Dry eye management in a Sjögren's syndrome mouse model by inhibition of p38-MAPK pathway. Diagn Pathol 2014; 9: 5
25. Liu Z, Chen D, Chen X, Bian F, Qin W, Gao N, Xiao Y, Li J, Pflugfelder SC, Li DQ. Trehalose induces autophagy against inflammation by activating TFEB signaling pathway in human corneal epithelial cells exposed to hyperosmotic stress. Invest Ophthalmol Vis Sci 2020; 61(10): 26
26. Zheng Q, Ren Y, Reinach PS, She Y, Xiao B, Hua S, Qu J, Chen W. Reactive oxygen species activated NLRP3 inflammasomes prime environment-induced murine dry eye. Exp Eye Res 2014; 125: 1–8
27. Dinarello CA. Immunological and inflammatory functions of the interleukin-1 family. Annu Rev Immunol 2009; 27(1): 519–550
28. Christofi M, Le Sommer S, Mölzer C, Klaska IP, Kuffova L, Forrester JV. Low-dose 2-deoxy glucose stabilises tolerogenic dendritic cells and generates potent *in vivo* immunosuppressive effects. Cell Mol Life Sci 2021; 78(6): 2857–2876
29. Zhang X, M VJ, Qu Y, He X, Ou S, Bu J, Jia C, Wang J, Wu H, Liu Z, Li W. Dry eye management: targeting the ocular surface microenvironment. Int J Mol Sci 2017; 18(7): 1398
30. deRoetth A Jr. Glycolytic activity of the cornea. AMA Arch Opthalmol 1951; 45(2): 139–148
31. Thies RS, Mandel LJ. Role of glucose in corneal metabolism. Am J Physiol 1985; 249(5): C409–C416
32. Chen X, Rao J, Zheng Z, Yu Y, Lou S, Liu L, He Q, Wu L, Sun X. Integrated tear proteome and metabolome reveal panels of inflammatory-related molecules via key regulatory pathways in dry eye syndrome. J Proteome Res 2019; 18(5): 2321–2330
33. Pucino V, Certo M, Bulusu V, Cucchi D, Goldmann K, Pontarini E, Haas R, Smith J, Headland SE, Blighe K, Ruscica M, Humby F, Lewis MJ, Kamphorst JJ, Bombardieri M, Pitzalis C, Mauro C. Lactate buildup at the site of chronic inflammation promotes disease by inducing $CD4^+$ T cell metabolic rewiring. Cell Metab 2019; 30(6): 1055–1074.e8
34. Hui S, Ghergurovich JM, Morscher RJ, Jang C, Teng X, Lu W, Esparza LA, Reya T, Le Zhan, Yanxiang Guo J, White E, Rabinowitz JD. Glucose feeds the TCA cycle via circulating lactate. Nature 2017; 551(7678): 115–118
35. Zhang JY, Zhou B, Sun RY, Ai YL, Cheng K, Li FN, Wang BR, Liu FJ, Jiang ZH, Wang WJ, Zhou D, Chen HZ, Wu Q. The metabolite α-KG induces GSDMC-dependent pyroptosis through death receptor 6-activated caspase-8. Cell Res 2021; 31(9): 980–997
36. Craig JP, Nichols KK, Akpek EK, Caffery B, Dua HS, Joo CK, Liu Z, Nelson JD, Nichols JJ, Tsubota K, Stapleton F. TFOS DEWS II definition and classification report. Ocul Surf 2017; 15(3): 276–283
37. López-Cano JJ, González-Cela-Casamayor MA, Andrés-Guerrero V, Herrero-Vanrell R, Benítez-Del-Castillo JM, Molina-Martínez IT. Combined hyperosmolarity and inflammatory conditions in stressed human corneal epithelial cells and macrophages to evaluate osmoprotective agents as potential DED treatments. Exp Eye Res 2021; 211: 108723
38. Chen H, Gan X, Li Y, Gu J, Liu Y, Deng Y, Wang X, Hong Y, Hu Y, Su L, Chi W. NLRP12- and NLRC4-mediated corneal epithelial pyroptosis is driven by GSDMD cleavage accompanied by IL-33 processing in dry eye. Ocul Surf 2020; 18(4): 783–794